Diagnostics for the General Fusion LM26 Machine

W. H. Gould[1], F. Braglia[1], P. Carle[1], A. Rohollahi[1], A. Radich[1], S. Coop[1], X. Feng[1], K. Martens[1]

[1]General Fusion Inc., Vancouver, British Columbia, Canada

25th Topical Conference on High Temperature Plasma Diagnostics, Asheville, North Carolina, USA, April 21-25, 2024, **Poster 4.2.22**

MTF Overview

General Fusion (GF) is pursuing Magnetized Target Fusion (MTF) technology to produce commercial fusion power. In this approach, a rotating liquid metal wall forms a vortex and vacuum cavity, into which a Marshall gun forms a magnetized spherical tokamak plasma. An array of pistons compresses the liner radially inwards, compressing the plasma to fusion conditions. Neutrons released from the deuterium-tritium fusion reaction deposit their energy into the liquid metal, which is circulated through a heat exchanger to generate steam to power a turbine to generate electricity.

Advantages:

- The liquid metal liner shields the machine structure from fusion neutrons.
- A liquid metal liner is expected to give a high tritium breeding ratio of 1-4-1.8 [1].
- The liquid metal can be pumped out of the vessel to extract heat for power generation.
- Mechanical compression is an economic way of heating the plasma.

Figure 1: Mockup of near commercial machine.

LM26 Overview

GF is building a machine called Lawson Machine 2026 (LM26) to demonstrate the physics viability of MTF, with goals to:

1. Compress a plasma to 10 keV by 2025
2. Achieve scientific breakeven equivalent by 2026

The target chamber's outer wall is a solid lithium liner within a cylindrical composite vacuum vessel. Toroidal coils outside the vessel are pulsed, creating a θ-pinch to compress the liner (Fig. 3), which will compress the plasma to fusion conditions. The duration of the compression is about 3 ms [2]. Liner diagnostics will measure the wall position during compression.

Between compression shots, the compressed lithium liner will be extracted and recycled. A fresh liner will be replaced, and the machine re-evacuated. The inner surfaces of the liner and target chamber will be evaporatively lithium coated. The initial and final plasma parameters are shown in Table 1. A veto will be implemented to ensure target initial plasma parameters are reached before compression. We expect to run compression shots once per week, beginning mid-2025. Compression trajectories from a simplified model are shown in Fig. 15.

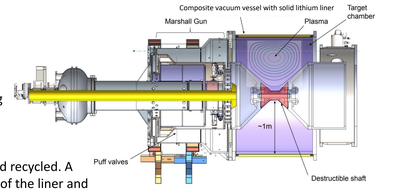

Figure 2: Cross section of LM26 vessel.

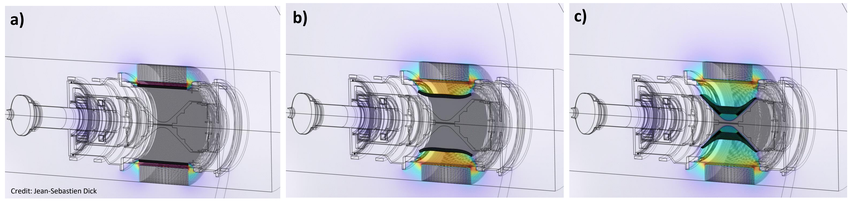

Figure 3: a) t=50us. The θ-pinch coils pulse, generating a high magnetic field on the back side of the solid liner. b) t=1600us. Magnetic pressure from the coil pulse initiates compression of the solid liner. c) t=2700us. The liner hits the cones and traps the plasma in the central volume around the shaft, achieving a peak radial compression ratio of 10:1 at t=3000us.

LM26 Diagnostic Ports:

Due to the solid lithium liner, no diagnostic ports are available on the outboard side of the plasma chamber, and access is limited to the central shaft. The central shaft has three distinct sections: the destructible equatorial section and the front and back cone sections (Fig. 4).

Six passive radiation/laser chords pass axially at four evenly spaced toroidal positions (Figs. 4,5). Port diameters are limited by structural and magnetic error field constraints, requiring ports closer to the destructible shaft (peak-compressed plasma position) to be smaller. Four other toroidal angles have normal-to-surface ports (Fig. 5).

An angled, 15 mm diameter, 2m long port through the shaft will provide an unobstructed view of the plasma core at peak compression (Fig. 6).

Table 1: LM26 plasma parameters for a 10 keV compression.

	Pre-compression	Peak compression
Major Radius	0.5 m	0.08 m
Minor Radius	0.4 m	0.03 m
Core Temperature	5e19 m^{-3}	1e23 m^{-3}
Core Density	0.5 T	100 T
Core B-field		

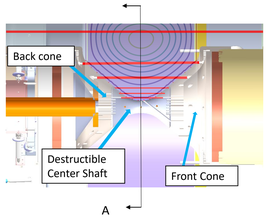

Figure 4: One set of six passive radiation and laser chords shown at one toroidal angle. There are four sets of these chords (Fig. 10).

LM26 Diagnostics

Thomson Scattering:

Thomson scattering will measure time-resolved core electron temperature at pre- and peak compression. For pre-compression, a 1064 nm burst laser will pass through the plasma to an ex-situ beam dump. Collection optics will likely be mounted on a re-entrant lens assembly, imaging the plasma core (Fig. 6).

The peak-compression measurement is under development. A beam dump to control stray light will be located inside the back cone section. We expect high levels of background from Bremsstrahlung and line radiation from the high n_e and T_e plasma. See Poster 4.2.1 [3] for more details.

Neutron Measurement:

Neutron counters will be placed outside LM26. MCNP simulations of the expected neutron flux from LM26 have been developed with the UKAEA. The results will be used to optimize the type, number, and location of these counters, and validate their responses. Fig. 7 shows a neutron flux map for an LM26 peak compression shot.

For a direct ion temperature measurement from fusion neutrons at peak compression, a neutron spectrometer is being developed in collaboration with SFU and TRIUMF (see *Diagnostic Collaborations*). Through the peak compression chord (Fig. 6), the neutron spectrometer measures neutrons' time of flight between two layers of scintillators to determine the neutron energy distribution, which is a function of the ion temperature [4]. See Poster 3.4.45 [5] for more details.

Interferometry:

A set of interferometer chords will be the primary measurement of electron density. For outer chords (early compression), we will use a CO2-HeNe (10.6um/633nm) system. For the inner chords at late compression, high density ($n_e = 10^{22} - 10^{23}\ m^{-3}$), we may use a shorter wavelength 1550/1310 nm system. This is due to beam refraction causing misalignment and the fast phase shift ramp requiring very high measurement bandwidth. See density trajectory (Fig. 15). Some chords must make two passes through the plasma using machine-mounted retro-reflectors. This has significant risk due to vibration from the compression. Delay mounted mirrors and two-colour vibration subtraction are under development as vibration mitigation techniques.

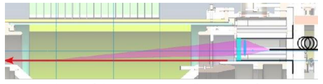

Figure 5: The axis of Thomson scattering collection optics for pre-compression must be ~10° from the laser, due to access constraints.

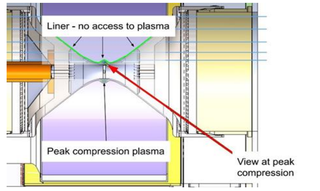

Figure 6: The Neutron and Xray Spectrometer view the plasma at peak compression through a 2m long, 15mm diameter port.

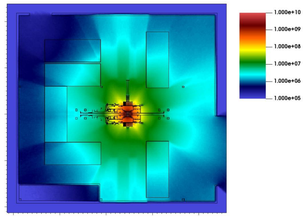

Figure 7: MCNP simulated neutron transport map for LM26 at peak compression, developed by the UKAEA.

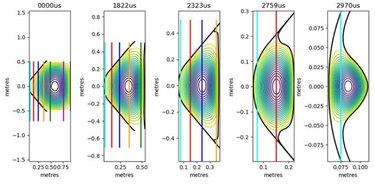

Figure 8: Grad-Shafranov equilibria at different compression times, overlayed with axial chords. Note how the liner collapse means axial views get blocked over the shot duration.

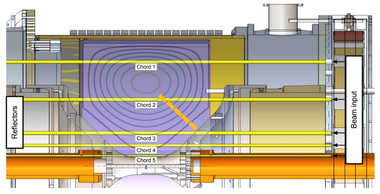

Figure 9: 5x axial interferometer chords passing through LM26 (yellow). Note, inner chords must double pass through the plasma. Orange dashes represent the probed reflectometer profile for a dual band (K and Ka band) system.

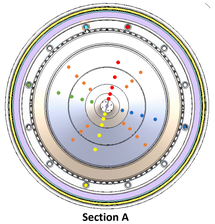

Section A

Figure 10: 4x sets of axial passive radiation/laser chords at different toroidal positions (green, red, yellow, blue). Normal-to-surface ports (Mirnov coils, 1x reflectometer) shown in orange.

Reflectometry:

A K-band, O-mode, homodyne reflectometer will be developed in collaboration with IST(see *Diagnostic Collaborations*) and mounted to the LM26 cone to measure edge electron density profiles from $n_e = 0.4 - 0.9 \times 10^{19}\ m^{-3}$. A custom horn will maximize directivity and power transmitted through the limited port diameter. Further development could upgrade to a dual-band, K- and Ka-band system, to measure density profiles from $0.4 - 2.0 \times 10^{19}\ m^{-3}$ (Fig. 9). Adding higher frequency bands to measure density profiles during compression (e.g. Q,U,V,W bands, up to $n_e = 1.5 \times 10^{20}\ m^{-3}$) is under consideration.

Survey Spectroscopy and Filterscopes:

There is risk that the collapsing lithium liner injects substantial impurities into the plasma. An array of survey spectrometers and fast-time-resolved filterscopes will measure the plasma impurity composition, targeting several lines of interest such as H_α, Li-I, Li-II.

Visible-UV Ion Doppler and Xray Spectroscopy:

An Ion Doppler Spectroscopy (IDS) system designed for UV-Visible range (e.g. Carbon V, 227 nm) will measure the pre-compression ion temperature. Above 400 eV, these lines will be fully ionized and UV-Visible IDS will not be possible. An X-ray imaging crystal spectroscopy system will be developed to measure the T_i and T_e at peak compression, using broadening and ratios of Ar, Ne and Fe impurity lines.

Magnetic Surface Probes:

Mirnov coils measuring the poloidal and toroidal magnetic field will be mounted on the cones and shaft. The probes are recessed within the shaft and surrounded by a thin metal shield to protect them from the plasma. This results in a strong frequency-dependent transfer function, which affects amplitude and phase of the incoming signal. The frequency response will be calibrated ex-situ with a dedicated device over a broad frequency range (~100 Hz-100 kHz).

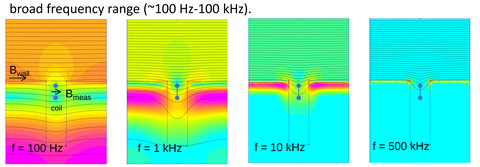

Figure 11: A simplified FEMM simulation shows that a conductive flux conserver results in a strong frequency dependence of the magnetic field strength measured by a Mirnov coil in a recessed well.

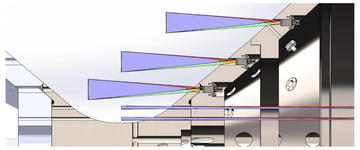

Figure 12: Cross-section of fields of view of cone-mounted AXUV diodes and front plate mounted AXUV.

AXUV Te Ratio and Bolometry:

Signal ratios from three filtered AXUV (absolute extreme ultraviolet) diodes provide view-cone average electron temperature measurements. The three filters are 6, 12 and 22 µm of Mylar, each with a 0.1 µm aluminum layer for visible spectrum absorption. For pre-compression, the diagnostic will be on the LM26 front cone, with a 10° view cone angle, for sufficient signal and spatial resolution (Fig. 12). Three filters are used to have three unique ratios for measuring T_e, which can be crosschecked against one another.

For peak compression, the diagnostic will be mounted on the front plate with an axial view through the front cone. The view cone angle is approximately 1° (Fig. 12). Thicker mylar filters (~12, 22, 40 µm) will be used for measuring bremsstrahlung at higher temperatures. High bremsstrahlung radiation at peak compression is expected to compensate for the small measurement solid angle. A fourth, unfiltered diode, with the same view will measure the broad-spectrum radiated power, from which total radiated power can be estimated. The diodes will likely be broken and replaced with each compression shot, so responsivity degradation is not expected to be an issue.

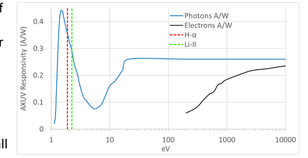

Figure 13: AXUV responsivity vs photon energy (blue). For filtered, varied response in lower energy spectrum can be disregarded. For unfiltered measurement, an assumption of effective diode responsivity must be made.

Diagnostic Challenges and Mitigations

- Temperature, density and magnetic field will change by several orders of magnitude during compression. Fast (~5 µs) diagnostics with high dynamic range are required.
- Access to plasma is mostly limited to the central shaft, and the compressing liner will cut off most access ports. Critical diagnostics will have dedicated access points.
- Shocks/vibration from compression may cause loss of alignment and damage to sensors. Vibration isolation and rapid replacement and calibration protocols are being designed.
- Windows/optics will be protected from lithium vapours via shutters, reentrant windows, or coatings.
- The machine will operate at UHV (10^{-7} torr) and high temperature (150 °C) during a compression shot to soften the lithium. Surface temperature of the shaft could be much higher near peak compression. Compatible materials are required for all plasma-facing components of all diagnostics systems.

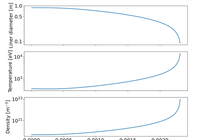

Figure 14: LM26 compression trajectories for some of the main physical parameters.

Diagnostic Collaborations

GF is collaborating with several international institutions to develop and improve multiple diagnostics, including:

- The UK Atomic Energy Authority, on the development of Thomson Scattering, magnetic probes manufacturing, and neutron measurement and validation
- TRIUMF, Canada's national particle accelerator centre, hosted on the campus of University of British Columbia and Simon Fraser University to develop the neutron spectrometer
- Instituto Superior Técnico (IST) at the University of Lisbon to develop a reflectometer to measure electron density profiles

References: [1] General Fusion TBR Analysis by UKAEA [internal report], March 17, 2024.
[2] F. Braglia et al, "Diagnostics for the General Fusion LM26 Machine," presented at the BRNMI Workshop, Washington, DC, USA, Jan 9-11, 2024.
[3] S. Coop et al., "4 kHz high-dynamic-range Thomson scattering on LM26," presented at High Temp. Plasma Diag. (HTPD) Conf., Asheville, NC, USC, April 22-25, 2024. Poster 4.2.1.
[4] P. Carle et al., "Neutron emission spectrometer to measure ion temperature on the Fusion Demonstration Plant", Rev. Sci. Instrum. 93, 113539 (2022).
[5] A. Radich et al., "Neutron Spectrometer and Neutron Counting Diagnostics for General Fusion's LM26 Machine," presented at High Temp. Plasma Diag. (HTPD) Conf., Asheville, NC, USC, April 22-25, 2024. Poster 3.4.45.